SQUEEZE EFFECTS OF AN INFINITELY LONG, RIGID CYLINDER ON A HIGHLY COMPRESSIBLE POROUS LAYER IMBIBED WITH LIQUID

Mihaela RADU[1], Traian CICONE[2]

Ex-poro-hydrodynamic (XPHD) lubrication describes the lifting effect produced by the flow of fluid through an extremely compressible porous material subjected to compression. Studies published recently on the behaviour of such materials, for various configurations, reveal good potential in shock absorption. The present study addresses the case of an infinitely long cylinder that impacts a highly compressible porous layer interposed between the cylinder and a rigid plane. Based on a 1D flow model, the lift effects for squeeze at constant speed, constant force and impact loading, respectively are analyzed.

Keywords: XPHD lubrication, porous layer, squeeze, cylinder on plane, impact

1. Introduction

Intuitively, we can visualize a porous medium as a complex system of cavities or capillaries, arbitrary distributed in a form that resembles a labyrinth. The fundamental problem of porous media is the complexity of the flow through this maze of capillaries which is practically impossible to solve analytically, and which will not describe globally the phenomena. This is why a macroscopic approach of the behaviour of the fluid inside the material is preferred.

A new mechanism of lubrication, based on highly compressible porous layers imbibed with liquids, was observed and studied by M. D. Pascovici [1] under the name of ex-poro-hidrodynamic (XPHD) lubrication. Similar results have been obtained in parallel by S. Weinbaum and R. Crawford, for porous materials with extremely high porosities imbibed with gases [2], [3]. Recently, the research team led by B. Bou-Saïd has published a series of papers on similar effects for planar configuration (disk-on-plane) where the effects of complex rheological fluid properties and fluid inertia have been investigated analytically and numerically [4], [5].

The lift effect is explained by the resistance to flow of the fluid forced to be expelled through the pores of the material subjected to compression. This

[1] Assist., Department of Machine Elements and Tribology, University POLITEHNICA of Bucharest, Romania, e-mail: mihaela.radu@upb.ro
[2] Prof., Department of Machine Elements and Tribology, University POLITEHNICA of Bucharest, Romania

mechanism can occur when the porous media imbibed with fluid is compressed between conformal/non-conformal contacts, for sliding or normal motion. For sliding motion, configurations like step or inclined surfaces [6] showed an increased lift effect in comparison with hydrodynamic conditions. Squeeze studies, for plane-on-plane contact ([7], [8]) sphere-on-plane ([8], [9]), inner contact of cylinder-on-cylinder ([10]) have a great potential.

The work reported in the present paper intends to validate the damping efects observed in previous articles, for a new configuration, of a cylinder-on-plane.The configuration studied in this article has originated from the interest in estimating the damping capabilities in mechanical application of impact or bio-articulations (as the knee joint) [11].

2. The model

A slice of the geometry of the contact between a rigid, infinitely long, impermeable cylinder and a porous layer imbibed with fluid, fixed on a rigid and impermeable support, parallel with the cylinder's axis, is represented in Fig. 1. The assumption that the cylinder axis is parallel to the plane, converts the model to an axisymmetric 1D model. The groundwork of XPHD lubrication model is presented extensively in [12].

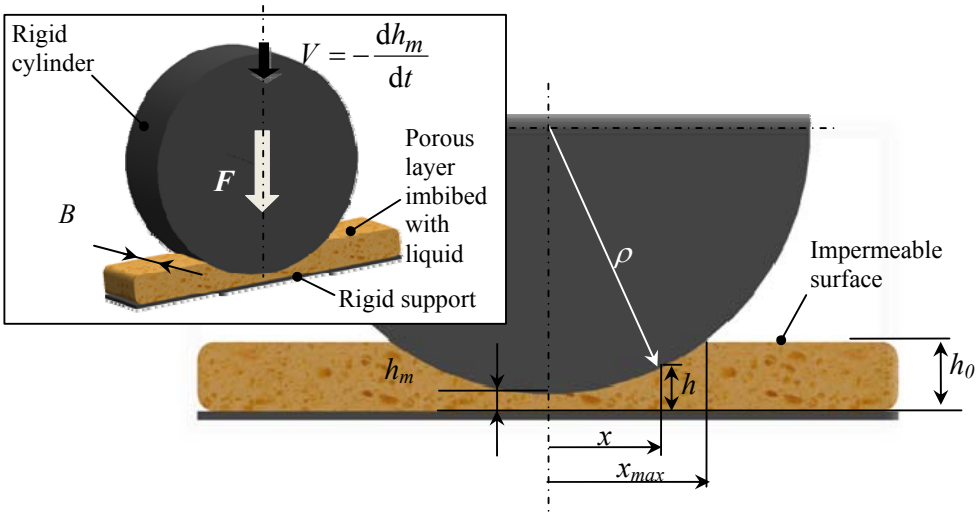

Fig. 1. The cylinder-on-plane geometry

For the mathematical modelling of the XPHD process is customary by all authors ([1]-[10], [12]) of this field that porous media of this type are Brinkman media, which, for low permeability can be approximated with Darcy media. The foundation of XPHD lubrication is based on a few simplifying hypothesis [13]:

- The porous layer is relatively thin, homogeneous and isotropic.
- The top surface of the porous layer is impermeable.
- The pressure is constant across the thickness of the porous layer.
- The liquid is Newtonian, the flow is laminar and isoviscous.
- The elastic forces of the compressed solid structure (also called porous matrix) are negligible compared to viscous forces.

Extremely compressible porous layers are characterized by *porosity* variation with deformation, and correspondingly, by a *permeability* variation. The notion of *solid fraction* is defined as the product between the thickness of the material, h, and the inverse of porosity, $1\text{-}\varepsilon$. Under compression, the geometry of the pores changes, squeezing out the fluid from the material, but the solid fraction remains constant if we suppose that the cross-section area normal to the direction of compression doesn't increase significantly:

$$(1-\varepsilon)h = (1-\varepsilon_0)h_0 \tag{1}$$

During compresion, the thickness in mid-plane, $h_m(t)$, varies from h_0 to $h_{\min}$ (see Fig. 1):

$$h_{\min} = (1-\varepsilon_0)h_0 \tag{2}$$

The strain, δ, is defined similar as in solid mechanics:

$$\delta(x,t) = 1 - h(x,t)/h_0 \tag{3}$$

Thus, the mid-plane strain becomes $\delta_m(t) = 1 - h_m(t)/h_0$ and the minimum mid-plane thickness is $1 - h_{\min}(t)/h_0 = \varepsilon_0$, which implies an interesting outcome: *the maximum strain, when compressing to $h_{\min}$, is equal to the initial porosity.*

At any given moment, the thickness of the porous layer is obtained from a simple geometry using the radius of the cylinder ρ and the thickness in the mid-plane $h_m(t) = h(x=0,t)$:

$$h(x,t) = h_m(t) + \rho - \sqrt{\rho^2 - x^2} \tag{4}$$

The *permeability* of the porous layer is associated to the porosity, ε, according with Kozeny-Carman law [12] - regularly used in previous studies ([1], [6]-[10], [12]):

$$\phi = \frac{D\varepsilon^3}{(1-\varepsilon)^2} \tag{5}$$

where D is a complex constant of the porous material, approximated as $D = d_f^{\,2}/16k$, d_f being the diameter of the material fibre and k, a constant arbitrary chosen between 5 and 10.

3. Numerical approach

The cylinder's length, B, is assumed to be large relative to its radius, so that side leakage can be neglected. One-dimensional finite volume simulations are carried out for the simplified model of an infinitely long cylinder. The mesh of the model using one element on the porous layer thickness (according to the assumption of constant pressure on porous layer) was split on x into m cells.

The pressure distribution and, consequently the generated lift force, yields from the flow rate conservation inside the porous material, which states that the volume of fluid dislocated by the cylinder is equal to the volume of fluid expelled on both sides of the cylinder, normal to the direction of compression (in-plane flow).

The conservation equation is discretized on each mesh element. The flow rate squeezed out of each cell $i = \overline{2,m}$, is equal with the in-plane flow rate flowing through the boundaries with neighbouring cells, i+1 and i-1 (Fig. 2):

$$q_i = q_{i+1} + q_{i-1} \tag{6}$$

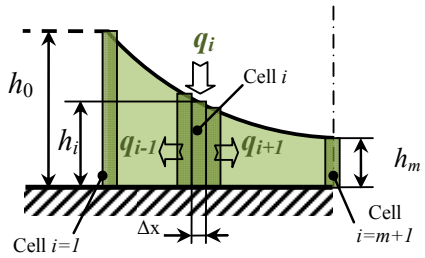

Fig. 2. Meshing of the porous domain

The volume displaced in unit time by compressing with velocity V an element i, of dimension Δx and porosity ε_i, is calculated as:

$$q_i = (\varepsilon_i \cdot \Delta x \cdot B) \cdot V \tag{7}$$

The in-plane flow rate through a neighbouring cell, considering mean thickness and permeability, is calculated using Darcy model:

$$q_{i\pm1} = \frac{\phi_{i\pm 1/2} \cdot h_{i\pm 1/2}}{\eta} \cdot B \cdot \left.\frac{\mathrm{d}p}{\mathrm{d}x}\right|_{i\pm1} \tag{8}$$

Combining eq. (6), (7) and (8), and using dimensionless parameters, the dimensionless pressure in cell i can be calculated using the pressures in the neighbouring cells:

$$\overline{p}_i = \frac{2\Delta\overline{x}^2 \cdot \varepsilon_i + \overline{p}_{i-1} \cdot \overline{\phi}_{i-1/2} \cdot \overline{h}_{i-1/2} + \overline{p}_{i+1} \cdot \overline{\phi}_{i+1/2} \cdot \overline{h}_{i+1/2}}{\overline{\phi}_{i-1/2} \cdot \overline{h}_{i-1/2} + \overline{\phi}_{i+1/2} \cdot \overline{h}_{i+1/2}}, i = \overline{2,m} \qquad (9)$$

The boundary condition of null pressure at $x=x_{max}$ ($i=1$), and symmetry condition for $x=0$ ($i=m+1$) give, in dimensionless form:

$$\overline{p}_1 = 0 \text{ and } \overline{p}_{m+1} = \overline{p}_m + \frac{2\Delta\overline{x}^2 \cdot \varepsilon_i}{\overline{\phi}_{i-1/2} \cdot \overline{h}_{i-1/2}} \qquad (10)$$

The dimensionless lift force is obtained as:

$$\overline{F} = 2\sqrt{\frac{2\rho}{h_0}}\left(\frac{\overline{p}_1}{2} + \frac{\overline{p}_{m+1}}{2} + \sum_{i=2}^{m} \overline{p}_i\right)\Delta\overline{x} \qquad (11)$$

The solution is obtained by Gauss-Seidel method with an over-relaxation coefficient of 1.99, until the relative pressure difference obtained between two consecutive steps is smaller than 10^{-6}.

The numerical code is written in FORTRAN language under Microsoft Visual Studio based on the above equations, for three loading cases: constant speed (V=ct), constant force (F=ct) and imposed impulse ($M \cdot V_0$=ct).

4. Results and discussions

4.1. Mesh size and time step

The results presented in this chapter are obtained with an original numerical code based on the model presented above with a mesh of 300 cells and 300 time steps. The mesh size influence was analyzed graphically by comparison with several mesh sizes with up to three times more cells and four times more time steps. The time of processing increases dramatically, while the relative errors in terms of force were acceptable - under 3%, except for large strains - due to the asymptotic variation of the force around zero porosity.

4.2. Constant speed squeeze (V = ct)

Despite its reduced practical interest, the numerical analysis for the case of constant speed squeeze represents the core of the next two cases.

The numerical algorithm for constant speed squeeze is developed with a constant step strain in the mid-plane. Because the contact width, x_{max}, is continuously increasing during compression, the mesh step Δx is modified at each time step. Using the thickness in the mid-plane and the width of the cylinder that is in contact with the porous layer, the pressure in each cell is calculated, and

consequently the force. The dimensionless form of the model allows the reduction of process variables to only two: the size ratio ρ/h_0 and the initial porosity ε_0.

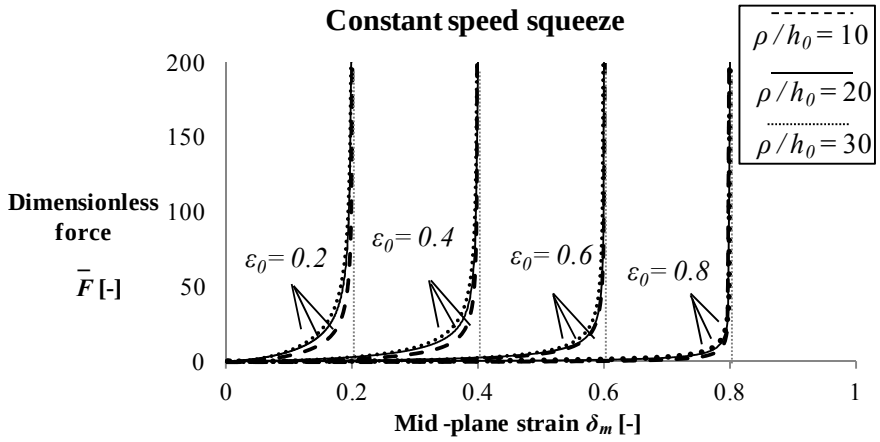

Fig. 3 Dimensionless force, $\bar{F}$ vs. mid-plane strain, δ_m, for different porosities ε_0 and size ratios ρ/h_0

In Fig. 3, the dimensionless force $\bar{F}$ is plotted with mid-plane strain for different initial porosities. The graph shows that the lower the porosity, the higher the force – a result similar with the sphere/plane [6] and disk/plane [6] configuration. It is obvious that the bigger the size ratio, the greater the force.

4.3. Constant force loading (F = ct)

The numerical algorithm for the constant force loading is based on the previous one (constant velocity), apart from the solution which is obtained iteratively until the force predicted is equal with the imposed one. The main squeeze parameters, the velocity and time, are calculated for constant compressions steps. The most important parameter is considered the duration of compression τ, which is the time to reach zero-porosity in the mid-plane. It is calculated as the sum of time steps, and gives an overview of the extension of the damping process.

The duration of squeeze process for different initial porosities is plotted in Fig. 4. The longest duration for the impacting cylinder to reach zero porosity, meaning the highest resistance to flow, is associated with an optimum porosity, found iteratively as $\varepsilon_{opt} = 0.26$. In sphere on plane configuration [6], similar results were found, with an optimum porosity of $\varepsilon_{opt} = 0.4$.

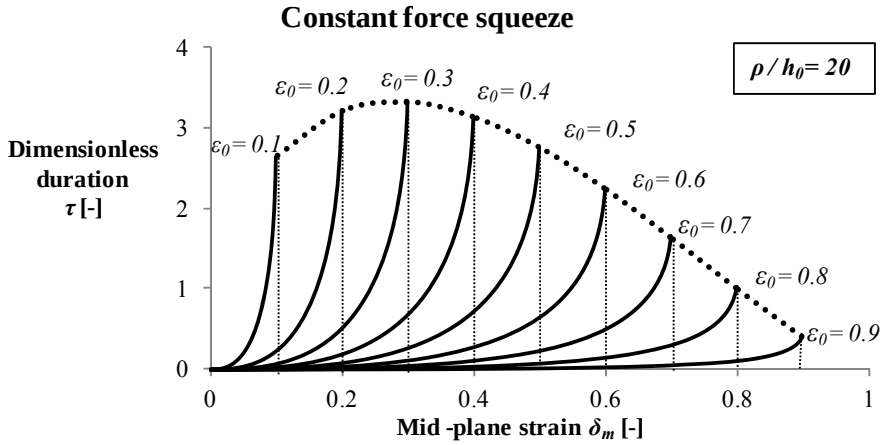

Fig. 4 Dimensionless duration, τ , vs. mid-plane strain, δ_m, for different porosities ε_0

4.4. Impact loading ($M \cdot V_0$=ct)

The squeeze under impact can be modelled based on the impulse conservation theory – neglecting inertial forces:

$$M \cdot \mathrm{d}V = -F \cdot \mathrm{d}t \tag{12}$$

The input parameter is the product between mass and velocity at contact, in dimensionless form, $\overline{M}$. Using a constant time step and an explicit time integration scheme, the current velocity is calculated using the acceleration obtained in dimensionless form from equation (12):

$$\overline{V}(\bar{t} + \Delta\bar{t}) = \overline{V}(\bar{t}) - \frac{\overline{F}(\bar{t})}{\overline{M}} \Delta\bar{t} \tag{13}$$

The mid-plane thickness is calculated using the average of the current and previous velocity:

$$\overline{h}_m(\bar{t} + \Delta\bar{t}) = \overline{h}_m(\bar{t}) - \Delta\bar{t} \cdot \frac{\overline{V}(t) + \overline{V}(\bar{t} + \Delta\bar{t})}{2} \tag{14}$$

The algorithm of compression is stopped either when the process is damped ($\overline{V}(t) = 0$) or it reaches $\varepsilon = 0$ in the mid-plane.

High energy impact is not damped entirely while compressing the porous material until full compaction, which is why the rigid body continues to move even after that, but this process in not relevant when obtaining the maximum load.

In Fig. 5, the impact force is represented with respect to different geometric ratios. In all of the cases plotted in Fig. 5 and Fig. 6 the impact is completely damped before full compression of the porous material (when δ_m=ε_0). What is interesting is that increasing 10 times the size ratio, the maximum force is just 25% greater.

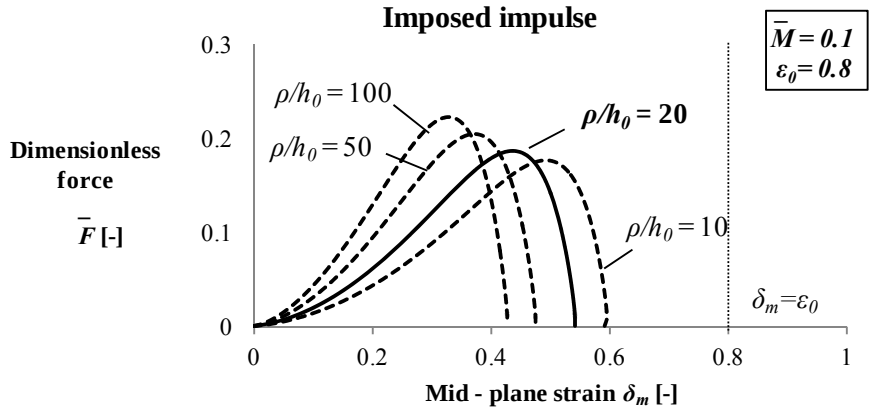

Fig. 5. Dimensionless impact force $\bar{F}$ vs. mid-plane strain, δ_m, for different size ratios ρ/h_0

In Fig. 6, the impact force is represented for different values of porosity, for a given impulse and geometry. The cases plotted here do not compress until the porosity reaches zero which means that the impact is fully damped.

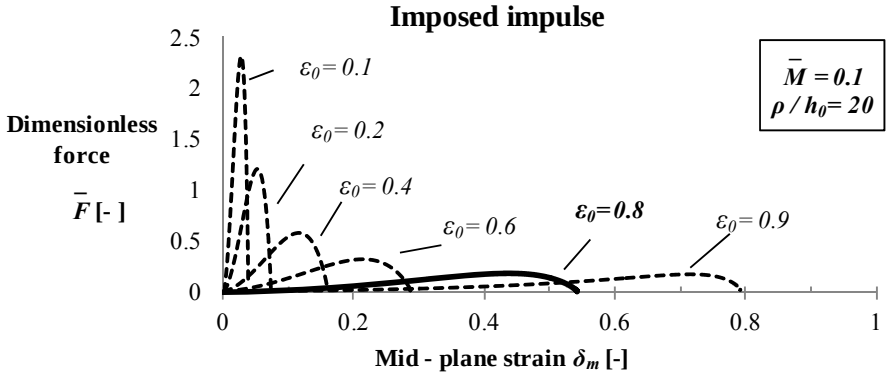

Fig. 6 Dimensionless impact force $\bar{F}$ vs. mid-plane strain, δ_m, for different porosities ε_0

In Fig. 7, is shown the method used to determine the maximum mass of impact. For a given case, where the porosity and the geometry is known, by testing different values of impact mass and analyzing the velocity variation, one can observe that the higher the impact mass, the higher the compression of the material. The maximum impact mass that can be damped, which is decelerated until zero velocity, is associated with the full compression of the porous zone, so when the strain $\delta_m = \varepsilon_0$. This was determined iteratively with one digit accuracy.

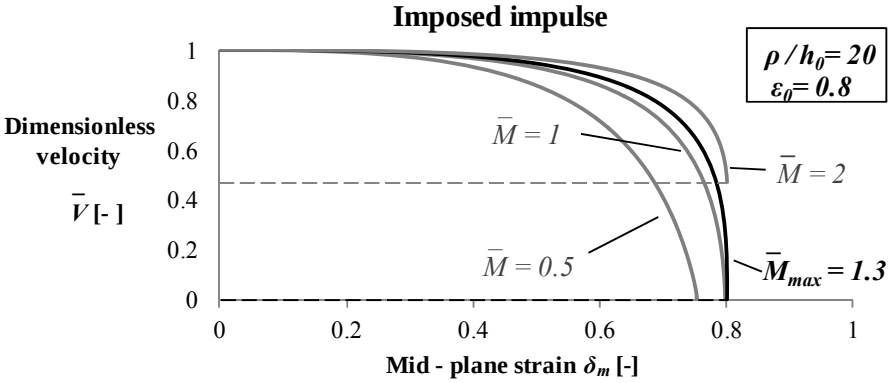

Fig. 7 Dimensionless impact velocity $\bar{v}$ vs. mid-plane strain, δ_m, for different dimensionless mass values, $\overline{M}$

The maximum damped mass for different values of initial porosity shown in dimensionless form in Fig. 8, has an optimum porosity between 0.3÷0.4.

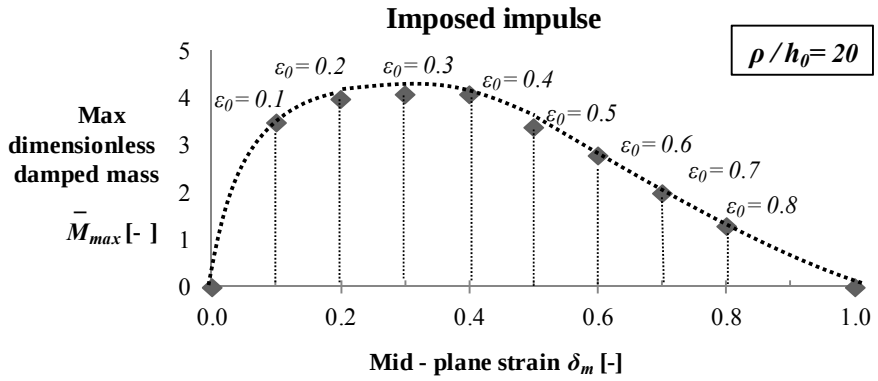

Fig. 8 Maximum dimensionless damped mass $\overline{M}$ vs. mid-plane strain, δ_m, for different porosities ε_0

5. Conclusions

The present paper analyzes a simplified model, 1D, of the squeeze effect of a fluid imbibed in an extremely compressible porous layer, produced by a rigid cylinder of large width with respect to its diameter. The model is based on the principles of ex-poro-hydrodynamic lubrication, with application in impact loadings, and the solution is obtained numerically.

The results presented demonstrate that one can achieve excellent

performances of damping for a cylinder-on-plane contact, just as for other configurations. Also, the influence of the most important parameters that define the process are studied. The parametric analysis in dimensionless form permits the fast and easy evaluation of the damping capacity depending on the material properties and contact dimensions.

This paper presents three scenarios of normal loading for ex-poro-hydrodynamic lubrication. The numerical study proves the existence of an optimum porosity that maximizes the damping effect in normal motion with constant force/impact loading and provides a practical guideline in terms of optimum porosity. Under constant force compression, an optimum initial porosity of the material, ε_{opt}, can be determined for a given geometrical configuration, from the longest time of squeeze. If the material is subjected to impact loading, the highest impact force is obtained for: low porosities, high imposed momentum and large radius of the cylinder with comparison to porous layer thickness. Depending on the geometrical configuration, one can obtain an optimum initial porosity of the material, ε_{opt}, that can damp the highest impact mass.

The model serves as reference for the evaluation of an analytical model, published in [13], to establish the accuracy of simplifying assumptions such as the parabolic approximation of the cylinder's boundary and Taylor series approximation of a *arctg* function. This model represents a first step to a more complex, 2D analysis of the contact.

Notations

B – length of the cylinder [m];
d_f – diameter of the material fiber [m];
D – complex constant of the porous material [m^2];
F – lift force [N];
$\overline{F} = \frac{FD}{\eta V B \rho h_0}$ – dimensionless lift force[-];
h – thickness of the porous material[m];
$\overline{h} = \frac{h}{h_0}$ – dimensionless thickness of the porous material[-];
i – mesh element [-];
k – constant in Kozeny-Carman law [-];
q – flow rate [m^3/s];
$\overline{q} = \frac{q}{BV\sqrt{2\rho h_0}}$ – dimensionless flow rate[-];
m – number of cells [-];

M – mass of the cylinder [kg];

$\overline{M} = \frac{MDV_0}{\eta B \rho {h_0}^2}$ – dimensionless mass of the cylinder [-];

p – pressure [Pa];

$\overline{p} = \frac{p \cdot D}{\eta \rho V}$ – dimensionless pressure [-];

t – time [s];

$\bar{t} = t \cdot \frac{v_0}{h_0}$ – dimensionless time [-];

V – normal velocity [m/s];

$\overline{V} = \frac{V}{V_0}$ – dimensionless velocity [-];

x – in-plane coordinate [m];

$\bar{x} = \frac{x}{\sqrt{2 \cdot \rho \cdot h_0}}$ – dimensionless in-plane coordinate [-];

Δx – mesh step [m];

ε – porosity [-];

η – fluid viscosity [Pa·s];

ρ – radius of the cylinder [m];

δ – strain [-];

$\tau = \frac{FDt}{\eta B \rho {h_0}^2}$ – dimensionless duration (for constant force squeeze) [-];

ϕ – permeability of the porous layer [m^2];

$\overline{\phi} = \frac{\phi}{D}$ – dimensionless permeability [-].

Subscripts

0 – initial;
m – mid-plane;
min – minimum;
opt – optimum.

R E F E R E N C E S

[1] *M. D. Pascovici*, "Procedure and device for pumping by fluid dislocation", Romanian patent no. 109469, 1994.

[2] *J. Feng, S.Weinbaum,* "Lubrication theory in highly compressible porous media: the mechanics of skiing, from red cells to humans", in J. of Fluid Mechanics, vol. 422, 2000, pp. 281-317.

[3] *R. Crawford, R. Nathan, L. Wang, Q. Wu,* "Experimental study on lift generation inside a random synthetic porous layer under rapid conpaction", in Experimental Thermal and Fluid Science, vol. 36, 2012, pp. 205-216

[4] *M. Nabhani, M. El Khlifi, B. Bou-Saïd*, "A numerical simulation of viscous shear effects on porous squeeze film using the Darcy-Brinkman model", in Mecanique and Indrustries, vol. 11 (5), 2010, pp. 327-337.

[5] *M. Nabhani, M. El Khlifi, B. Bou-Saïd*, "A generalized model for porous flow in squeezing film situations", in Lubrication Science, vol. 22(2), 2010, pp. 37-53.

[6] *M. D. Pascovici,* "Lubrication processes in highly compressible porous layers, Lubrification et tribologie des revetements minces", in Actes des journees internationales francophones de tribologie (JIFT 2007), Poitiers University, Presses Polytechniques et Universitaires Romandes, vol. 1, 2007, pp. 3-12.

[7] *M. D. Pascovici, T. Cicone, V. Marian*, "Squeeze process under impact, in highly compressible porous layers, imbibed with liquids", in Tribology International, vol. 42, 2009, pp.1433-1438.

[8] *M. D. Pascovici, T. Cicone, "*Squeeze-film of unconformal, compliant and layered contacts", in Tribology International, vol. 36, no.11, 2003, pp. 791-99.

[9] *M. D. Pascovici, T. Cicone, V. Marian, "*Impact of a rigid sphere on a highly compressible porous layer imbibed with a Newtonian liquid", in Tribology International, vol. 42, 2009, pp. 1433-1438.

[10] *M. B. Ilie, M. D. Pascovici, V. G. Marian,* "Squeeze processes in narrow circular damper with highly compressible porous layer imbibed with liquids", in Proceedings IMechE Part J: J. of Engineering Tribology, vol. 225(6), 2011, pp. 539-549.

[11] *M. Berli, D. Campana, S. Ubal, J. Di Paolo,* "Lubrication model of a knee prosthesis, with non Newtonian fluid and porous rough material", in Latin American Applied Research, vol. 39, 2009, pp. 105-111.

[12] *M. D. Pascovici,* "Lubrication by Dislocation: A New Mechanism for Load Carrying Capacity", in Proceedings of 2nd World Tribology Congress, Vienna(Paper on CD) , 2001, pp. 41-48.

[13] A.E. Scheidegger, "The physics of flow through porous media", University of Toronto Press, 3rd edition, pp. 141, 1974.

[14] *M. Radu, T. Cicone,* "Constant speed squeeze process in XPHD conditions - cylinder on plane configuration", Proceed. of the16th Intern. Conf. on EHD Lubrication and Traction, Suceava, 2012, pp. 86-90.